Available online at http://ijim.srbiau.ac.ir/
Int. J. Industrial Mathematics (ISSN 2008-5621)
Vol. 8, No. 2, 2016 Article ID IJIM-00694, 16 pages
Research Article

Non-Newtonian thermal convection of eyring-powell fluid from an isothermal sphere with biot number effects

S. Abdul Gaffar *†, V. Ramachandra Prasad ‡, E. Keshava Reddy §

Received Date: 2015-05-05 Revised Date: 2015-07-30 Accepted Date: 2015-12-09

Abstract

This article investigates the nonlinear, steady boundary layer flow and heat transfer of an incompressible Eyring-Powell non-Newtonian fluid from an isothermal sphere with Biot number effects. The transformed conservation equations are solved numerically subject to physically appropriate boundary conditions using a second-order accurate implicit finite-difference Keller Box technique. The influence of a number of emerging dimensionless parameters, namely the Eyring-Powell rheological fluid parameter (ε), the local non-Newtonian parameter based on length scale (δ), Prandtl number (Pr), Biot number (γ) and dimensionless tangential coordinate (ξ) on velocity and temperature evolution in the boundary layer regime are examined in detail. Furthermore, the effects of these parameters on surface heat transfer rate and local skin friction are also investigated. It is found that the velocity and heat transfer rate (Nusselt number) decrease with increasing (ε), whereas temperature and skin friction increase. An increasing (δ) is observed to enhance velocity, local skin friction and heat transfer rate but reduces the temperature. An increase (γ) is seen to increase velocity, temperature, local skin friction and Nusselt number. The study is relevant to chemical materials processing applications.

Keywords : Non-Newtonian Eyring-Powell fluid model; Isothermal sphere; Finite difference numerical method; Boundary layers; Biot number.

Nomenclature

a radius of the sphere
C_f skin friction coefficient
C fluid parameter
f non-dimensional steam function
Gr Grashof number
g acceleration due to gravity
Nu heat transfer rate
Pr Prandtl number
$r(x)$ radial distance from symmetrical axis to surface of the sphere
T temperature of the fluid
u, v non-dimensional velocity components along the x- and y - directions, respectively
V velocity vector
x stream wise coordinate
y transverse coordinate

Greek

α Thermal diffusivity
β Fluid parameter
η The dimensionless radial coordinate
μ Dynamic viscosity
ν Kinematic viscosity

*Corresponding author. abdulsgaffar0905@gmail.com
†Department of Mathematics, Jawaharlal Nehru Technological University Anantapur, Anantapuramu-515002, India.
‡Department of Mathematics, Madanapalle Institute of Technology and Sciences, Madanapalle-517325, India.
§Department of Mathematics, Jawaharlal Nehru Technological University Anantapur, Anantapuramu-515002, India.

θ The dimensionless temperature
ρ Density of non-Newtonian fluid
ξ The dimensionless tangential coordinate
Ψ Dimensionless stream function
ε Fluid parameter
γ Biot number

Subscripts
w conditions on the wall (sphere surface)
∞ Free stream conditions

1 Introduction

Non-Newtonian transport phenomena arise in many branches of chemical and materials processing engineering. Examples of such fluids include coal-oil slurries, shampoo, paints, clay coating and suspensions, grease, cosmetic products, custard, physiological liquids (*blood, bile, synovial fluid*) etc. Non-Newtonian fluids are handled extensively by chemical industries namely plastics and polymer. The classical equations employed in simulating Newtonian viscous flows i.e. the Navier Stokes equations fail to simulate a number of critical characteristics of non-Newtonian fluids. The relationship between the shear stress and rate of strain in such fluids are very complicated in comparison to viscous fluids. The viscoelastic features in non-Newtonian fluids add more complexities in the resulting equations when compared with Navier Stokes equations. Significant attention has been directed at mathematical and numerical simulation of non-Newtonian fluids. Recent investigations have implemented, respectively the Casson model[38], Second-order Reiner-Rivlin differential fluid models [32], Power-law nanoscale models [44], Tangent Hyperbolic fluid models [4], Jeffrey's viscoelastic model [5] and Third grade fluid model [24, 39].
Convective heat transfer has also mobilized substantial interest owing to its importance in industrial and environmental technologies including energy storage, gas turbines, nuclear plants, rocket propulsion, geothermal reservoirs, photovoltaic panels etc. The convective boundary condition has also attracted some interest and this usually is simulated via a Biot number in the wall thermal boundary condition. Ishak [22]discussed the similarity solutions for flow and heat transfer over a permeable surface with convective boundary condition. Aziz [13] provided a similarity solution for laminar thermal boundary layer over a flat surface with a convective surface boundary condition. Aziz [14] further studied hydrodynamic and thermal slip flow boundary layers with an iso-flux thermal boundary condition. The buoyancy effects on thermal boundary layer over a vertical plate subject a convective surface boundary condition was studied by Makinde and Olanrewaju [26]. Further recent analyses include Makinde and Aziz [27]. Gupta et al. [19] used a variational finite element to simulate mixed convective-radiative micropolar shrinking sheet flow with a convective boundary condition. Swapna et al. [43] studied convective wall heating effects on hydromagnetic flow of a micropolar fluid. Makinde et al. [28] studied cross diffusion effects and Biot number influence on hydromagnetic Newtonian boundary layer flow with homogenous chemical reactions and MAPLE quadrature routines. Bg et al. [11] analyzed Biot number and buoyancy effects on magnetohydrodynamic thermal slip flows. Subhashini et al. [41] studied wall transpiration and cross diffusion effects on free convection boundary layers with a convective boundary condition.
An interesting non-Newtonian model developed for chemical engineering systems is the Eyring-Powell fluid model. This rheological fluid model has certain advantages over the other non-Newtonian formulations, including simplicity, ease of computation and physical robustness. Firstly it is deduced from kinetic theory of liquids rather than the empirical relation. Additionally, it correctly reduces to Newtonian behavior for low and high shear rates. Eyring-Powell fluid model [33], a complete mathematical model proposed by Powell and Eyring in 1944. Several communications utilizing the Eyring Powell fluid model have been presented in the scientific literature. Malik et al. [29] presented boundary layer flow of an Eyring Powell model fluid due to a stretching cylinder with variable viscosity. Eldabe et al. [18] studied numerical study of viscous dissipation effect on free convection heat and mass transfer of MHD Eyring Powell fluid flow through a porous medium. Javed et al. [23] investigated flow of an Eyring Powell non-Newtonian fluid over a stretching sheet. Characteristics of heat-

ing scheme and mass transfer on the peristaltic flow an Eyring Powell fluid in an endoscope was discussed by Nadeem et al. [6]. Akbar et al. [7] implemented the Eyring-Powell model for peristaltic thermal convection flows of reactive biofluids; Hayat et al. [20] studied the steady flow of an Eying-Powell fluid over a moving surface with convective boundary conditions. Asmat Ara et al. [12] implemented the Eyring-Powell fluid to study the radiation effects over an exponentially shrinking sheet. K.V. Prasad et al. [34] examined the boundary layer flow of a non-Newtonian Eyring-Powell fluid over a non-isothermal stretching sheet. A.M. Siddiqui [40] examined the thin film flow of an Eyring-Powell fluid on a vertically moving belt.

In many chemical engineering and nuclear process systems, curvature of the vessels employed is a critical aspect of optimizing thermal performance. Examples of curved bodies featuring in process systems include torus geometries, wavy surfaces, cylinders, cones, ellipses, oblate spheroids and in particular, spherical geometries, the latter being very popular for storage of chemicals and also batch reactor processing. Heat transfer from spheres has therefore mobilized much attention among chemical engineering researchers who have conducted both experimental and computational investigations for both Newtonian and non-Newtonian fluids. Bg et al. [10] examined the free convection magnetohydrodynamic flow from a sphere in porous media using network simulation, showing that temperatures are boosted with magnetic field and heat transfer is enhanced from the lower stagnation point towards the upper stagnation point. Prhashanna and Chhabra [37] obtained numerical solutions for streamline and temperature contours in heat transfer from a heated sphere immersed in quiescent power-law fluids, showing that shear-thinning behaviour may elevate heat transfer rates by three hundred percent, whereas shear-thickening depletes heat transfer rates by 30 to 40% compared with Newtonian fluids. Further interesting investigations of heat transfer from spheres have been presented by Dhole et al. [17] for forced convection in power-law fluids using the finite volume method and by Bg et al. [9] for combined heat and species diffusion in micropolar fluids with cross-diffusion effects. Prasad et al. [35] have also studied radiative heat flux effects on magneto-convective heat and species diffusion from a sphere in an isotropic permeable medium. Molla et al. [31] studied the effect of temperature dependent viscosity on MHD natural convection flow from an isothermal sphere using implicit finite difference method. M. Miraj et al. [30] examined the effects of viscous dissipation and radiation on magnetohydrodynamic free convection flow along a sphere with joule heating and heat generation. Recent study on sphere includes [4, 5]. V.R. Prasad et al. [2] studied the free convection flow and heat transfer on non-Newtonian Tangent Hyperbolic fluid from an isothermal sphere with partial slip. Ramachandra Prasad et al. [3] examined the non-similar computational solutions for free convection boundary layer flow of a Nanofluid from an isothermal sphere in a non-Darcy porous medium using Keller-Box method.

The objective of the present study is to investigate the laminar boundary layer flow and heat transfer of an Eyring-Powell non-Newtonian fluid from an isothermal sphere. The non-dimensional equations with associated dimensionless boundary conditions constitute a highly nonlinear, coupled two-point boundary value problem. Keller's implicit finite difference scheme is implemented to solve the problem [3]. The effects of the emerging thermophysical parameters, namely the rheological parameters (ε), Biot number (γ) and Prandtl number (Pr), on the velocity, temperature, local skin friction, and heat transfer rate (local Nusselt number) characteristics are studied. The present problem has to the authors knowledge not appeared thus far in the scientific literature and is relevant to polymeric manufacturing processes in chemical engineering.

2 Non-Newtonian Constitutive Eyring-Powell Fluid Model

In the present study a subclass of non-Newtonian fluids known as the Eyring-Powell fluid is employed owing to its simplicity. The Cauchy stress tensor, in an Eyring-Powell non-Newtonian fluid [33] takes the form:

$$\tau_{ij} = \mu \frac{\partial u_i}{\partial x_j} + \frac{1}{\beta} sinh^{-1}\left(\frac{1}{C}\frac{\partial u_i}{\partial x_j}\right) \qquad (2.1)$$

where μ is dynamic viscosity, β and C are the rheological fluid parameters of the Eyring-Powell

fluid model. Consider the second-order approximation of the $sinh^{-1}$ function as:

$$sinh^{-1}\left(\frac{1}{C}\frac{\partial u_i}{\partial x_j}\right) \cong$$

$$\frac{1}{C}\frac{\partial u_i}{\partial x_j} - \frac{1}{6}\left(\frac{1}{C}\frac{\partial u_i}{\partial x_j}\right)^3, \left|\frac{1}{C}\frac{\partial u_i}{\partial x_j}\right| \ll 1 \qquad (2.2)$$

The introduction of the appropriate terms into the flow model is considered next. The resulting boundary value problem is found to be well-posed and permits an excellent mechanism for the assessment of rheological characteristics on the flow behaviour.

3 Mathematical Flow Model

Steady, double-diffusive, laminar flow of an Eyring-Powell fluid from an isothermal sphere, is considered, as illustrated in Fig. 1. The x-coordinate is measured along the surface of an isothermal sphere from the lowest point and the y-coordinate is measured normal to the surface, with a denoting the radius of the sphere. $r(x) = asin\left(\frac{x}{a}\right)$ is the *radial distance* from the symmetrical axis to the surface of the sphere. The gravitational acceleration g, acts downwards. We also assume that the Boussineq approximation holds i.e. that density variation is only experienced in the buoyancy term in the momentum equation. Both isothermal sphere and the Eyring-Powell fluid are maintained initially at the same temperature. Instantaneously they are raised to a temperature $T_w > T_\infty$, the ambient temperature of the fluid which remains unchanged. Introducing the boundary layer approximations and in line with approaches of [41, 33, 29], the equations for mass, momentum, and energy, can be written as follows:

$$\frac{\partial(ru)}{\partial x} + \frac{\partial(rv)}{\partial y} = 0 \qquad (3.3)$$

$$u\frac{\partial u}{\partial x} + v\frac{\partial u}{\partial y} = \left(\nu + \frac{1}{\rho\beta C}\right)\frac{\partial^2 u}{\partial y^2} - \frac{1}{2\rho\beta C^3}\left(\frac{\partial u}{\partial y}\right)^2\frac{\partial^2 u}{\partial y^2} + g\beta_1 sin\left(\frac{x}{a}\right)(T - T_\infty) \qquad (3.4)$$

$$u\frac{\partial T}{\partial x} + v\frac{\partial T}{\partial y} = \alpha\frac{\partial^2 T}{\partial y^2} \qquad (3.5)$$

where u and v are the velocity components in the x - and y - directions respectively and all the other terms are defined in the nomenclature. The Eyring-Powell fluid model therefore introduces a mixed derivative (second order, second degree) into the momentum boundary layer equation (3.4). The non-Newtonian effects feature in the shear terms only of eqn. (3.4) and not the convective (acceleration) terms. The third term on the right hand side of eqn. (3.4) represents the thermal buoyancy force and couples the velocity field with the temperature field eqn. (3.5).

$$\begin{aligned} &At\ y = 0,\ u = 0,\ v = 0, \\ &-k\frac{\partial T}{\partial y} = h_w(T_w - T) \\ &As\ y \to \infty,\ u \to 0,\ T \to T_\infty \end{aligned} \qquad (3.6)$$

Here T_∞ is the free stream temperture, k is the thermal conductivity, h_w is the convective heat transfer coefficient, T_w is the convective fluid temperature. The stream function Ψ is defined by

$$ru = \frac{\partial(r\Psi)}{\partial y} \qquad and \qquad rv = -\frac{\partial(r\Psi)}{\partial x}$$

and therefore, the continuity equation is automatically satisfied. In order to render the governing equations and the boundary conditions in dimensionless form, the following non-dimensional quantities are introduced.

$$\begin{aligned} &\xi = \frac{x}{a},\ \eta = \frac{y}{a}Gr^{\frac{1}{4}},\ f = \frac{\Psi}{\nu\xi}Gr^{-\frac{1}{4}}, \\ &\theta(\xi,\eta) = \frac{T - T_\infty}{T_w - T_\infty}, Pr = \frac{\nu}{\alpha},\ \varepsilon = \frac{1}{\mu\beta C}, \\ &Gr = \frac{g\beta a^3(t_w - T_\infty)}{\nu^2}, \delta = \frac{\nu^2}{2C^2a^4}Gr^{3/2} \end{aligned} \qquad (3.7)$$

In view of the transformation defined in eqn. (3.7), the boundary layer eqns. (3.4) - (3.6) reduce to the following *fifth* order system of coupled, nonlinear, dimensionless partial differential equations for momentum and energy for the regime:

$$(1+\varepsilon)f''' + (1 + \xi cot\xi)ff'' - \left(f'\right)^2 + \theta\frac{sin\xi}{\xi} - \varepsilon\partial\xi^2\left(f''\right)^2 f''' = \xi\left(f'\frac{\partial f'}{\partial\xi} - f''\frac{\partial f}{\partial\xi}\right) \qquad (3.8)$$

$$\frac{\theta''}{Pr} + (1 + \xi cot\xi)\, f\theta' = \xi \left(f' \frac{\partial \theta}{\partial \xi} - \theta' \frac{\partial f}{\partial \xi} \right) \tag{3.9}$$

The transformed dimensionless boundary conditions are:

$$At\ \eta = 0,\ f = 0,\ f' = 0,\ \theta = 1 + \frac{\theta'}{\gamma}$$
$$As\ \eta \to 0,\ f' \to 0,\ \theta \to 0 \tag{3.10}$$

Here primes denote the differentiation with respect to η and $\gamma = \frac{ah_w}{k} Gr^{\frac{-1}{4}}$ is the Biot number. The wall thermal boundary condition in (3.10) corresponds to convective cooling. The skin-friction coefficient (shear stress at the sphere surface) and Nusselt number (heat transfer rate) can be defined using the transformations described above with the following expressions.

$$Gr^{\frac{-3}{4}} C_f =$$

$$(1 + \varepsilon)\, \xi f''(\xi, 0) - \frac{\delta}{3} \varepsilon \xi^3 \left(f''(\xi, 0) \right)^3 \tag{3.11}$$

$$Gr^{\frac{-1}{4}} Nu = -\theta'(\xi, 0) \tag{3.12}$$

The location, $\xi \sim 0$, corresponds to the vicinity of the *lower stagnation point* on the sphere. Since $\frac{sin\,\xi}{\xi} \to \frac{0}{0}$ i.e. 1. For this scenerio, the model defined by eqns. (3.8) - (3.9) contracts to an *ordinary* differential boundary value problem:

$$(1.0 + \varepsilon)\, f''' + f f'' - \left(f' \right)^2 + \theta = 0 \tag{3.13}$$

$$\frac{1}{Pr} \theta'' + f\theta' = 0 \tag{3.14}$$

The general model is solved using a powerful and unconditionally stable finite difference technique introduced by Keller [21]. The Keller-box method has a second order accuracy with arbitrary spacing and attractive extrapolation features.

4 Numerical Solution with Keller Box Implict Method

The Keller-Box implicit difference method is implemented to solve the nonlinear boundary value problem defined by eqns. (3.8)-(3.9) with boundary conditions (3.10). This technique, despite recent developments in other numerical methods, remains a powerful and very accurate approach for parabolic boundary layer flows. It is unconditionally stable and achieves exceptional accuracy [21]. Recently, this method has been deployed in resolving many challenging, multi-physical fluid dynamics problems. These include hydromagnetic Sakiadis flow of non-Newtonian fluids [42], nanofluid transport from a horizontal cylinder [1], radiative rheological magnetic heat transfer [15], waterhammer modelling [45], tangent hyperbolic fluid [2], Jeffrey's fluid [5] and magnetized viscoelastic stagnation flows [25]. The Keller-Box discretization is *fully coupled* at each step which reflects the physics of parabolic systems - which are also fully coupled. Discrete calculus associated with the Keller-Box scheme has also been shown to be fundamentally different from all other mimetic (physics capturing) numerical methods, as elaborated by Keller [21]. The Keller Box Scheme comprises four stages:

(1) Decomposition of the Nth order partial differential equation sywtem to N first order equations.

(2) Finite Difference Discretization.

(3) Quasilinearization of Non-Linear Keller Algebraic Equations and finally.

(4) Block-tridiagonal Elimination solution of the Linearized Keller Algebraic Equations.

Stage 1: Decomposition of Nth order partial differential equation system to N first order equations

Eqns.(3.8)-(3.9) subject to the boundary conditions (3.10) are first cast as a multiple system of first order differential equations. New dependent variables are introduced:

$$u(x, y) = f',\ v(x, y) = f'',\ t(x, y) = \theta' \tag{4.15}$$

These denote the variables for velocity, temperature and concentration respectively. Now Eqns.(3.8)-(3.9) are solved as a set of fifth order simultaneous differential equations:

$$f' = u \tag{4.16}$$

$$u^{'} = v \tag{4.17}$$

$$\theta^{'} = t \tag{4.18}$$

$$(1+\varepsilon)\, v^{'} + (1+\xi cot\xi)\, fv - u^2 - \varepsilon\partial\xi^2 v^2 v^{'} + s\frac{sin\xi}{\xi} = \xi\left(u\frac{\partial u}{\partial\xi} - u\frac{\partial f}{\partial\xi}\right) \tag{4.19}$$

$$\frac{t^{'}}{Pr} + (1+\xi cot\xi)\, ft = \xi\left(u\frac{\partial s}{\partial\xi} - t\frac{\partial f}{\partial\xi}\right) \tag{4.20}$$

where primes denote differentiation with respect to the variable, η. In terms of the dependent variables, the boundary conditions assume the form:

$$At\ \eta = 0,\ f = 0,\ u = 0,\ s = 1 + \frac{t}{\gamma}$$
$$As\ \eta \to 0,\ u \to 0,\ s \to 0 \tag{4.21}$$

Stage 2: Finite Difference Discretization

A two dimensional computational grid is imposed on the ξ-η plane as depicted in Fig. 2. The stepping process is defined by:

$$\eta_0 = 0, \eta_j = \eta_{j-1} + h_j, j = 1, 2, ..., J, \quad \eta_J \equiv \eta_\infty \tag{4.22}$$

$$\xi^0 = 0, \xi^n = \xi^{n-1} + k_n, n = 1, 2, ..., N \tag{4.23}$$

wherek_n is the $\Delta\xi$ − spacing and h_j is the $\Delta\eta$ − spacing.

If g_j^n denotes the value of any variable at (η_j, ξ^n), then the variables and derivatives of eqns. (4.16)-(4.20) at $\left(\eta_{j-1/2}, \xi^{n-1/2}\right)$ are replaced by:

$$g_{j-1/2}^{n-1/2} = \frac{1}{4}\left(g_j^n + g_{j-1}^n + g_j^{n-1} + g_{j-1}^{n-1}\right) \tag{4.24}$$

$$\left(\frac{\partial g}{\partial\eta}\right)_{j-1/2}^{n-1/2} = \frac{1}{2h_j}\left(g_j^n - g_{j-1}^n + g_j^{n-1} - g_{j-1}^{n-1}\right) \tag{4.25}$$

$$\left(\frac{\partial g}{\partial\xi}\right)_{j-1/2}^{n-1/2} = \frac{1}{2k^n}\left(g_j^n - g_{j-1}^n + g_j^{n-1} - g_{j-1}^{n-1}\right) \tag{4.26}$$

The finite-difference approximation of eqns. (4.16)-(4.20) for the mid-point $\left(\eta_{j-1/2}, \xi^n\right)$ are:

$$h_j^{-1}\left(f_j^n,\ f_{j-1}^n\right) = u_{j-1.2}^n \tag{4.27}$$

$$h_j^{-1}\left(u_j^n,\ u_{j-1}^n\right) = v_{j-1/2}^n \tag{4.28}$$

$$h_j^{-1}\left(s_j^n,\ s_{j-1}^n\right) = t_{j-1/2}^n \tag{4.29}$$

$$(1+\varepsilon)\left(v_j - v_{j-1}\right) - (1+\alpha)\frac{h_j}{4}\left(u_j + u_{j-1}\right)^2 + (1+\alpha+\xi cot\xi)\frac{h_j}{4}\left(f_j + f_{j-1}\right)\left(v_j + v_{j-1}\right) - \xi^2\frac{\varepsilon\delta}{4}\left(v_j + v_{j-1}\right)^2\left(v_j - v_{j-1}\right) + \frac{Bh_j}{2}\left(s_j + s_{j-1}\right) + \frac{\alpha h_j}{2}v_{j-1}^{n-1}\left(f_j + f_{j-1}\right) - \frac{\alpha h_j}{2}f_{j-1}^{n-1}\left(v_j + v_{j-1}\right) = [R_1]_{j-1/2}^{n-1} \tag{4.30}$$

$$\frac{1}{Pr}\left(t_j - t_{j-1}\right) - \frac{\alpha h_j}{4}\left(u_j + u_{j-1}\right)\left(s_j + s_{j-1}\right) + (1+\alpha+\xi cot\xi)\frac{h_j}{4}\left(f_j + f_{j-1}\right)\left(t_j + t_{j-1}\right) + \frac{\alpha h_j}{2}s_{i-1/2}^{n-1}\left(u_j + u_{j-1}\right) - \frac{\alpha h_j}{2}u_{i-1/2}^{n-1}\left(s_j + s_{j-1}\right) - \frac{\alpha h_j}{2}f_{i-1/2}^{n-1}\left(t_j + t_{j-1}\right) + \frac{\alpha h_j}{2}t_{i-1/2}^{n-1}\left(f_j + f_{j-1}\right) = [R_r]_{j-1/2}^{n-1} \tag{4.31, 4.32}$$

where we have used the abbreviations

$$\alpha = \frac{\xi^{n-1/2}}{k_n}, \qquad B = \frac{sin\ \xi^{n-1/2}}{\xi^{n-1/2}} \tag{4.33}$$

$$-h_j[(1+\varepsilon)\left(v^{'}\right)_{j-1/2}^{n-1} - (1-\alpha)\left(u^2\right)_{j-1/2}^{n-1} + (1-\alpha+\xi cot\xi)\left(fv\right)_{j-1/2}^{n-1} + Bs_{j-1/2}^{n-1} - \varepsilon\delta\xi^2\left(v^2\right)_{j-1/2}^{n-1}\left(v^{'}\right)_{j-1/2}^{n-1}] \tag{4.34}$$

$$[R_2]_{j-1/2}^{n-1} = -h_j[\frac{1}{Pr}\left(t^{'}\right)_{j-1/2}^{n-1} + \alpha\left(us\right)_{j-1/2}^{n-1} + (1-\alpha+\xi\ cot\ \xi)\left(ft\right)_{j-1/2}^{n-1}] \tag{4.35}$$

The boundary conditions are:

$$f_0^n = u_0^n = 0,\ s_0^n = 1,\ u_J^n = 0,\ v_J^n = 0,\ s_J^n = 0 \tag{4.36}$$

Table 1: Values of C_f and Nu for different ε and Pr ($\delta = 0.1, \gamma = 0.3, \xi = 1.0$).

Pr	$\varepsilon = 0.0$		$\varepsilon = 0.3$		$\varepsilon = 0.5$		$\varepsilon = 0.7$	
0	C_f	Nu	C_f	Nu	C_f	Nu	C_f	Nu
7	0.3573	0.5975	0.3859	0.5654	0.4024	0.5484	0.4172	0.5337
10	0.3319	0.6623	0.3581	0.6258	0.3730	0.6064	0.3865	0.5898
15	0.3046	0.7426	0.3281	0.7006	0.3416	0.6784	0.3537	0.6595
25	0.2725	0.8552	0.2930	0.8055	0.3048	0.7794	0.3154	0.7572
50	0.2331	1.0311	0.2503	0.9697	0.2601	0.9375	0.2689	0.9101
75	0.2124	1.1482	0.2278	1.0790	0.2366	1.0428	0.2446	1.0120
100	0.1986	1.2384	0.2129	1.1632	0.2211	1.1240	0.2285	1.0906

Table 2: Values of C_f and Nu for different ε and Pr ($\delta = 0.1, \gamma = 0.3, \xi = 1.0$).

Pr	$\varepsilon = 1.0$		$\varepsilon = 2.0$		$\varepsilon = 3.0$	
0	C_f	Nu	C_f	Nu	C_f	Nu
7	0.4371	0.5151	0.4904	0.4707	0.5314	0.4410
10	0.4047	0.5688	0.4532	0.5189	0.4905	0.4856
15	0.3700	0.6355	0.4136	0.5787	0.4471	0.5411
25	0.3297	0.7291	0.3678	0.6628	0.3971	0.6190
50	0.2808	0.8756	0.3126	0.7946	0.3370	0.7413
75	0.2553	0.9733	0.2838	0.8825	0.3058	0.8229
100	0.2384	1.0487	0.2649	0.9504	0.2853	0.8859

Table 3: Values of C_f and Nu for different δ and Pr ($\delta = 0.1, \gamma = 0.3, \xi = 1.0$).

Pr	$\delta = 0.0$		$\delta = 5$		$\delta = 10$		$\delta = 15$	
0	C_f	Nu	C_f	Nu	C_f	Nu	C_f	Nu
7	0.3675	0.5857	0.3669	0.5873	0.3663	0.5891	0.3657	0.5910
10	0.3412	0.6488	0.3408	0.6504	0.3403	0.6521	0.3399	0.6539
15	0.3130	0.7271	0.3126	0.7287	0.3123	0.7303	0.3120	0.7320
25	0.2798	0.8369	0.2796	0.8383	0.2794	0.8398	0.2791	0.8414
50	0.2393	1.0084	0.2391	1.0097	0.2390	1.0111	0.2389	1.0125
75	0.2179	1.1226	0.2178	1.1238	0.2177	1.1251	0.2176	1.1264
100	0.2037	1.2106	0.2036	1.2118	0.2035	1.2130	0.2034	1.2142

Table 4: Values of C_f and Nu for different δ and Pr ($\delta = 0.1, \gamma = 0.3, \xi = 1.0$).

Pr	$\delta = 20$		$\delta = 25$		$\delta = 30$	
0	C_f	Nu	C_f	Nu	C_f	Nu
7	0.3651	0.5930	0.3646	0.5954	0.3633	0.5977
10	0.3394	0.6559	0.3390	0.6580	0.3386	0.6604
15	0.3116	0.7338	0.3113	0.7358	0.3110	0.7379
25	0.2789	0.8431	0.2787	0.8448	0.2785	0.8466
50	0.2387	1.0139	0.2386	1.0154	0.2385	1.0169
75	0.2175	1.1277	0.2174	1.1291	0.2173	1.1305
100	0.2034	1.2154	0.2033	1.2167	0.2032	1.2180

Stage 3: Quasilinearization of Non-Linear Keller Algebraic Equations

Assuming f_j^{n-1}, u_j^{n-1}, v_j^{n-1}, s_j^{n-1}, t_j^{n-1} to be known for $0 \leq j \leq J$, then eqns.(4.27)-(4.31) constitute a system of $5J + 5$ equations for the solution of $5J + 5$ unknowns f_j^n, u_j^n, v_j^n, s_j^n, $t_j^n, j =$

Table 5: Numerical Values of $f''(\xi,0)$ (in brackets) and Skin Friction Coefficient C_f for different δ and ε.

$\frac{\delta}{\varepsilon}$	0.0	0.2	0.4	0.6	0.8	1.0
0.0	0.4406	0.4687	0.4936	0.5159	0.5363	0.5551
		(0.3906)	(0.3525)	(0.3225)	(0.2980)	(0.2776)
0.1	0.4406	0.4687	0.4935	0.5158	0.5362	0.5550
		(0.3909)	(0.3529)	(0.3225)	(0.2983)	(0.2779)
0.2	0.4406	0.4686	0.4934	0.5158	0.5362	0.5549
		(0.3912)	(0.3533)	(0.3232)	(0.2987)	(0.2782)
0.3	0.4406	0.4686	0.4934	0.5157	0.5361	0.5549
		(0.3915)	(0.3537)	(0.3236)	(0.2990)	(0.2785)
0.4	0.4406	0.4685	0.4933	0.5156	0.5360	0.5548
		(0.3918)	(0.3540)	(0.3240)	(0.2994)	(0.2788)
0.5	0.4406	0.4685	0.4932	0.5155	0.5359	0.5547
		(0.3921)	(0.3544)	(0.3243)	(0.2997)	(0.2792)
0.6	0.4406	0.4684	0.4931	0.5155	0.5358	0.546
		(0.3924)	(0.3548)	(0.3247)	(0.3001)	(0.2795)
0.7	0.4406	0.4684	0.4931	0.5154	0.5358	0.5545
		(0.3927)	(0.3552)	(0.3251)	(0.3005)	(0.2798)
0.8	0.4406	0.4683	0.4930	0.5153	0.5357	0.5545
		(0.3930)	(0.3556)	(0.3255)	(0.3008)	(0.2802)
0.9	0.4406	0.4683	0.4929	0.5152	0.5356	0.5544
		(0.3933)	(0.3560)	(0.3259)	(0.3012)	(0.2805)
10	0.4406	0.4682	0.4929	0.5151	0.5355	0.5543
		(0.3936)	(0.3564)	(0.3263)	(0.3016)	(0.2808)

$0, 1, 2, ..., J$. This non-linear system of algebraic equations is linearized by means of Newtons method as explained in [2, 3].

Stage 4: Block-tridiagonal Elimination Solution of Linear Keller Algebraic Equations

The linearized system is solved by the *block − elimination* method, since it possesses a block-tridiagonal structure. The bock-tridiagonal structure generated consists of *block matrices*. The complete linearized system is formulated as a *block matrix system*, where each element in the coefficient matrix is a matrix itself, and this system is solved using the efficient Keller-box method. The numerical results are strongly influenced by the number of mesh points in both directions. After some trials in the η -direction (radial coordinate) a larger number of mesh points are selected whereas in the ξ direction (tangential coordinate) significantly less mesh points are utilized. η_{max} has been set at 15 and this defines an adequately large value at which the prescribed boundary conditions are satisfied. ξ_{max} is set at 3.0 for this flow domain. Mesh independence is achieved in the present computations. The numerical algorithm is executed in **MATLAB** on PC. The method demonstrates excellent stability, convergence and consistency, as elaborated by Keller [21].

5 Numerical results and Interpretation

Comprehensive solutions have been obtained and are presented in Tables 1-5 and Figs. 3-9. The numerical problem comprises two independent variables (ξ, η), two dependent fluid dynamic variables (f, θ) and five thermo-physical and body force control parameters, namely, $\gamma, \delta, \varepsilon, Pr, \xi$. The following default parameter values i.e. $\gamma = 0.3, \delta = 0.1, \varepsilon = 0.1, Pr = 0.71, \xi = 1.0$ are prescribed (unless otherwise stated). Furthermore, the influence of stream-wise (transverse) coordinate on heat transfer characteristics is also investigated.

In Table 1 and 2 we present the influence of the Eyring-Powell fluid parameter, ε, on the skin friction and heat transfer rate, along with a variation in Prandtl number (Pr). With increasing ε, the skin friction is enhanced. The parameter ε is inversely proportional to the dynamic viscosity of the non-Newtonian fluid. There as ε is elevated, viscosity will be reduced and this will

induce lower resistance to the flow at the surface of the sphere i.e. accelerate the flow leading to an *escalation* of shear stress. Furthermore, this trend is sustained at any Pr. However, an increase in Pr markedly reduces the shear stress magnitudes. Similarly increasing ε is observed to reduce heat transfer rates, again at all Pr values, whereas it strongly accentuates heat transfer rates. Magnitudes of shear stress are always positive indicating that flow reversal (backflow) never arises.

Tables 3 and 4 document results for the influence of the local non-Newtonian parameter (based on length scale x) i.e. δ and also the Pr on skin friction and heat transfer rate. Skin friction is generally decreased with increasing δ. However heat transfer rate (i.e. local Nusselt number function) is found to be enhanced with increasing δ. $\delta = \frac{\nu^2}{2C^2a^4}Gr^{3/2}$ and inspection of this definition shows that the direct proportionality of δ to kinematic viscosity ν (with all other parameters being maintained constant) will generate a strong resistance to the flow leading to a deceleration i.e. drop in shear stresses. Conversely, the direct proportionality of δ to $Grashofnumber(Gr)$ will imply that thermal buoyancy forces are enhanced as δ increases and this will cause a boost in heat transfer by convection from the sphere surface manifesting with the greater heat transfer rates observed in Tables 3 and 4. These tables also show that with an increase in the Pr, the skin friction is also depressed whereas the heat transfer rate is elevated.

Table 5 presents the Keller box numerical values of the missing condition $f''(\xi, 0)$ (in brackets) and skin friction C_f for various values of δ and ε. It is found that skin friction is reduced with increasing values of δ.

Furthermore, the skin friction C_f is observed to be increased with a rise in the Eyring-Powell fluid parameter ε for all values of the local non-Newtonian parameter δ.

Fig. 3 - 4 illustrates the effect of Eyring-Powell fluid parameter ε, on the velocity $\left(f'\right)$ and temperature (θ) distributions through the boundary layer regime. Velocity is significantly decreased with increasing ε at larger distance from the sphere surface owing to the simultaneous drop in dynamic viscosity. Conversely, temperature is consistently enhanced with increasing values of ε The mathematical model reduces to the *Newtonian viscous flow model as* $\varepsilon \to 0$ *and* $\delta \to 0$. The momentum boundary layer equation in this case contracts to the familiar equation for Newtonian mixed convection from a sphere, viz

$$f''' + (1 + \xi cot\xi)\, f f'' - \left(f'\right)^2 + \theta \frac{sin\xi}{\xi} = \xi \left(f' \frac{\partial f'}{\partial \xi} - f'' \frac{\partial f}{\partial \xi} \right) \tag{5.37}$$

The thermal boundary layer equation (9) remains unchanged. In fig. 4 temperatures are clearly minimized for the Newtonian case ($\varepsilon = 0$) and maximized for the strongest non-Newtonian case ($\varepsilon = 3.0$)

Fig. 5 - 6 depict the velocity $\left(f'\right)$ and temperature (θ) distributions with increasing local non-Newtonian parameter δ. Very little tangible effect is observed in fig. 5, although there is a very slight increase in velocity with increase in δ. Similarly there is only a very slight depression in temperature magnitudes in Fig. 6 with a rise in δ.

Fig. 7 - 8 depict the evolution velocity $\left(f'\right)$ and temperature (θ) functions with a variation in Biot number, γ. Dimensionless velocity component (Fig. 7) is considerably enhanced with increasing γ. In fig. 8, an increase in γ is seen to considerably enhance temperatures throughout the boundary layer regime. For $\gamma < 1$ i.e. small Biot numbers, the regime is frequently designated as being "thermally simple" and there is a presence of more uniform temperature fields inside the boundary layer and the sphere solid surface. For $\gamma > 1$ thermal fields are anticipated to be non-uniform within the solid body. The Biot number effectively furnishes a mechanism for comparing the conduction resistance within a solid body to the convection resistance external to that body (offered by the surrounding fluid) for heat transfer. We also note that a Biot number in excess of 0.1, as studied in Figs. 7, 8 corresponds to a "thermally thick" substance whereas Biot number less than 0.1 implies a "thermally thin" material. Since γ is inversely proportional to thermal conductivity (k), as γ increases, thermal conductivity will be reduced at the sphere surface and this will lead to a decrease in the rate of heat transfer from the boundary layer to within the solid sphere, manifesting in a rise in temperature at the sphere surface and in the body of the

fluid - the maximum effect will be sustained at the surface, as witnessed in fig. 8. However for a fixed wall convection coefficient and thermal conductivity, Biot number as defined in $\gamma = \frac{xh_w}{k}Gr^{-1/4}$ is also directly inversely proportional to the local Grashof (free convection) number. As local Grashof number increases generally the enhancement in buoyancy causes a deceleration in boundary layer flows [37, 36, 16]; however as Biot number increases, the local Grashof number must decreases and this will induce the opposite effect i.e. accelerate the boundary layer flow, as shown in Fig. 7.

Fig. 9 - 10 depict the evolution velocity $\left(f'\right)$ and temperature (θ) distributions with dimensionless radial coordinate, for various transverse (stream wise) coordinate values, ξ. Generally velocity is noticeably lowered with increasing migration from the leading edge i.e. larger ξ values (Fig. 9). The maximum velocity is computed at the *lower stagnation point* $(\xi \sim 0)$ for *low values* of radial coordinate (η). The transverse coordinate clearly exerts a significant influence on momentum development. A very strong increase in temperature as observed in Fig. 10, is generated throughout the boundary layer with increasing ξ values. The temperature field decays monotonically. Temperature is maximized at the surface of the spherical body ($\eta = 0$, for all ξ) and minimized in the free stream ($\eta = 15$). Although the behaviour at the upper stagnation point $(\xi \sim \pi)$ is not computed, the pattern in fig. 6b suggests that temperature will continue to progressively grow here compared with previous locations on the sphere surface (lower values of ξ).

Fig. 11 - 12 show the influence of Eyring-Powell fluid parameter,ε on dimensionless skin friction coefficient $(1+\varepsilon)\,\xi f''(\xi,0) - \frac{\delta\varepsilon}{3}\xi^3\left(f'''(\xi,0)\right)^3$ and heat transfer rate $-\theta'(\xi,0)$ at the sphere surface. It is observed that the dimensionless skin friction is increased with the increase in ε i.e. the boundary layer flow is accelerated with decreasing viscosity effects in the non-Newtonian regime. Conversely, the surface heat transfer rate is substantially decreased with increasing ε values. Decreasing viscosity of the fluid (induced by increasing the ε value) reduces thermal diffusion as compared with momentum diffusion. A decrease in heat transfer rate at the wall will imply less heat is convected from the fluid regime to the sphere, thereby heating the boundary layer and enhancing temperatures.

Fig. 13 - 14 illustrates the influence of the local non-Newtonian parameter, δ , on the dimensionless skin friction coefficient and heat transfer rate. The skin friction (Fig. 13) at the sphere surface is accentuated with increasing , however only for very large values of the transverse coordinate, ξ. The flow is therefore strongly accelerated along the curved sphere surface far from the lower stagnation point. Heat transfer rate (local Nusselt number) is enhanced with increasing δ again at large values of ξ, as computed in Fig. 14.

Fig. 15 - 16 presents the influence of the Biot number, γ on the dimensionless skin friction coefficient and heat transfer rate at the sphere surface. The skin friction at the sphere surface is found to be greatly increased with rising γ values. This is principally attributable to the decrease in Grashof (free convection) number which results in an acceleration in the boundary layer flow, as elaborated by Chen and Chen [16]. Heat transfer rate (local Nusselt number) is enhanced with increasing γ , at large values of ξ, as computed in Fig. 16.

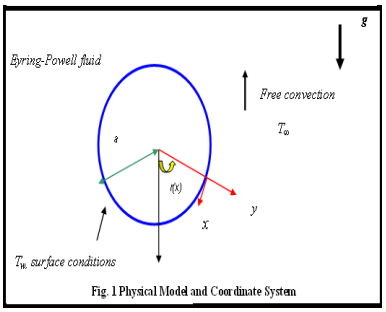

Figure 1: .

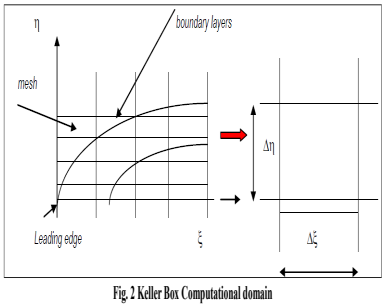

Figure 2: .

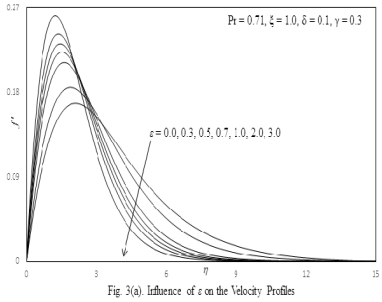

Figure 3: .

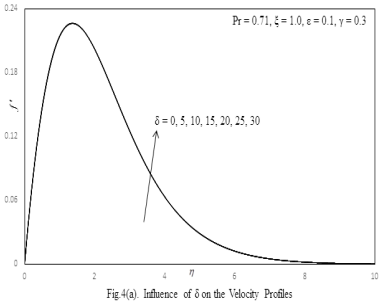

Figure 5: .

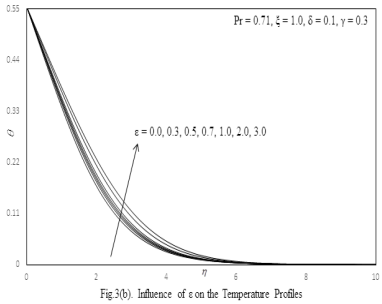

Figure 4: .

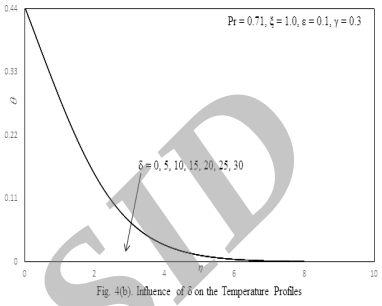

Figure 6: .

6 Conclusion

Numerical solutions have been presented for the buoyancy-driven flow and heat transfer of Eyring-Powell flow external to an isothermal sphere. The Keller-box implicit second order accurate finite difference numerical scheme has been utilized to efficiently solve the transformed, dimensionless velocity and thermal boundary layer equations, subject to realistic boundary conditions. Excellent correlation with previous studies has been demonstrated testifying to the validity of the present code. The computations have shown that:

(I) Increasing Eyring-Powell fluid parameter, ε, reduces the velocity and skin friction (surface shear stress) and heat transfer rate, whereas it elevates temperatures in the boundary layer.

(II) Increasing local non-Newtonian parameter, δ , increases the velocity, skin friction and Nusselt number for all values of radial coordinate i.e., throughout the boundary layer regime whereas it depresses temperature.

(III) Increasing Biot number, γ , increases velocity, temperature and skin friction (surface shear stress).

(IV) Increasing transverse coordinate, ξ generally decelerates the flow near the sphere surface and reduces momentum boundary layer thickness whereas it enhances temperature and therefore increases thermal boundary layer thickness in Eyring-Powell non-Newtonian fluids.

Generally very stable and accurate solutions are obtained with the present finite difference code. The numerical code is able to solve nonlinear boundary layer equations very efficiently and therefore shows excellent promise in simulating transport phenomena in other non-Newtonian fluids. It is therefore presently being employed to study micropolar fluids [19, 43] and viscoplastic fluids [8] which also simulate accurately many chemical engineering working fluids in curved geometrical systems.

References

[1] S. Abdul gaffar, V. Ramachandra Prasad, O. Anwar Beg, *Heat and mass transfer of Nanofluid from horizontal cylinder to micropolar fluid*, AIAA - Journal of Thermophysics and heat transfer 29 (2015) 127-139, http://dx.doi.org/10.2514/1.T4396/.

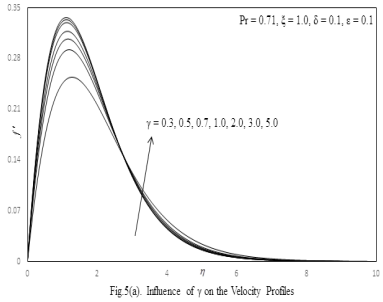

Figure 7: .

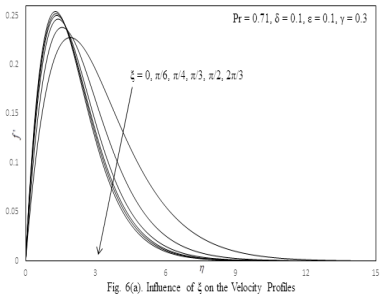

Figure 9: .

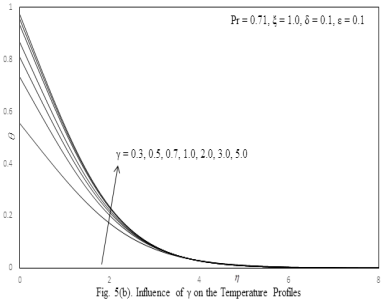

Figure 8: .

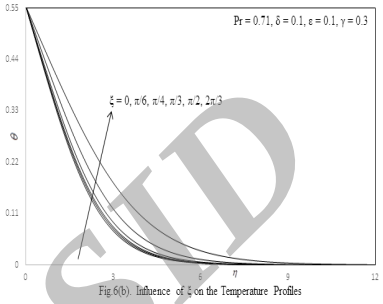

Figure 10: .

[2] S. Abdul gaffar, V. Ramachandra Prasad, E. Keshava Reddy, O. Anwar Beg, *Free convection flow and heat transfer on non-Newtonian Tangent Hyperbolic fluid from an isothermal sphere with partial slip*, Arabian Journal for Science and Engineering 39 (2014) 8157-8174, http://dx.doi.org/10.1007/s13369-014-1310-5/.

[3] S. Abdul gaffar, V. Ramachandra Prasad, O. Anwar Beg, *Non-similar computational solutions for free convection boundary layer flow of a Nanofluid from an isothermal sphere in a non-Darcy porous medium*, Journal of Nanofluids 4 (2015) 1-11, http://dx.doi.org/10.1166/jon.2015.1149/.

[4] S. Abdul gaffar, V. Ramachandra Prasad, O. Anwar Beg, *Numerical study of flow and heat transfer of non-Newtonian Tangent Hyperbolic fluid from a sphere with Biot number effects*, Alexandria Engineering Journal 54 (2015) 829-841, http://dx.doi.org/10.1016/j.aej.2015.07.001/.

[5] S. Abdul gaffar, V. Ramachandra Prasad, E. Keshava Reddy, O. Anwar Beg, *Thermal radiation and heat generation/absorption effects on viscoelastic double-diffusive convection from an isothermal sphere in porous media*, Ain Shams Engineering Journal 6 (2015) 1009-1030 http://dx.doi.org/10.1016/j.asej.2015.02.014/.

[6] N. S. NAkbar, S. Nadeem, *Characteristics of heating scheme and mass transfer on the peristaltic flow for an Eyring Powell fluid in an endoscope*, Int. J Heat Mass Transfer 55 (2012) 375-383, http://dx.doi.org/10.1016/j.ijheatmasstransfer.2011.09.029/.

[7] N. S. Akbar, S. Nadeem, T. Hayat, A. A. Hendi, *Simulation of heating scheme and chemical reactions on the peristaltic flow of an Eyring-Powell fluid*, Int. J. Numerical Methods for Heat and Fluid Flow 22 (2012) 764-776, http://dx.doi.org/10.1108/09615531211244907/.

[8] O. Anwar B, D. Tripathi, J-L. Curiel-Sosa, T-K. Hung, *Peristaltic propulsion of viscoplastic rheological materials, Advances in Biological Modelling*, Editor- T. Y. Wu, Taylor and Francis, Philadelphia, USA (2014).

[9] O. Anwar B, V. R. Prasad, B. Vasu, N. Bhaskar Reddy, Q. Li, R. Bhargava, *Free convection heat and mass transfer from an isothermal sphere to a*

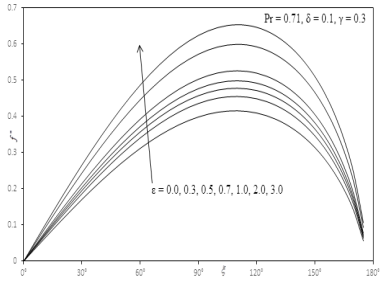

Fig. 7(a). Influence of ε on the Skin Friction

Figure 11: .

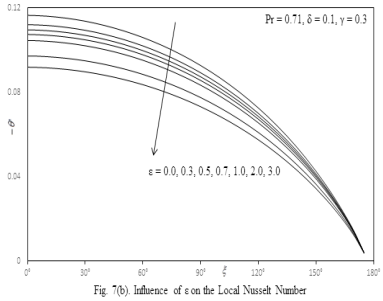

Fig. 7(b). Influence of ε on the Local Nusselt Number

Figure 12: .

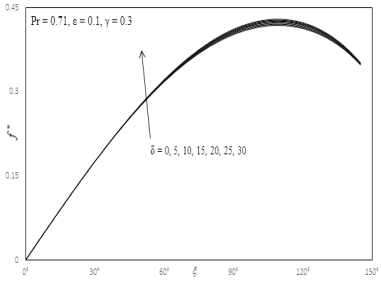

Fig.8(a). Influence of δ on the Skin Friction

Figure 13: .

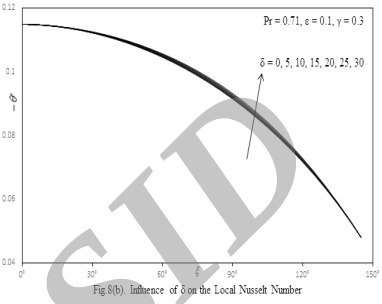

Fig.8(b). Influence of δ on the Local Nusselt Number

Figure 14: .

micropolar regime with Soret/Dufour effects, Int. J. Heat and Mass Transfer 54 (2011) 9-18. http://dx.doi.org/10.1016/j.ijheatmasstransfer.2010.10.005/.

[10] O. Anwar B, J. Zueco, R. Bhargava, H. S. Takhar, *Magnetohydrodynamic convection flow from a sphere to a non-Darcian porous medium with heat generation or absorption effects: network simulation*, Int. J. Thermal Sci. 48 (2009) 913-921, doi: http://dx.doi.org/10.1007/s13369-014-1310-5/.

[11] O. Anwar B, M. J. Uddin, M. M. Rashidi, N. Kavyani, *Double-diffusive radiative magnetic mixed convective slip flow with Biot number and Richardson number effects*, J. Engineering Thermophysics 23 (2014) 79-97, http://dx.doi.org/10.1134/S1810232814020015/.

[12] A. Asmat, Najeeb Alam Khan, Hassam Khan, Faqiha Sultan, *Radiation effect on boundary layer flow of an Eyring-Powell fluid over an exponentially shrinking sheet*, Ain Shams Engineering Journal, 5 (2014) 1337-1342, http://dx.doi.org/10.1016/j.asej.2014.06.002/.

[13] A. Aziz, *A similarity solution for laminar thermal boundary layer over a flat plate with a convective surface boundary condition*, Comm. Non. Sci. Num. Sim. 14 (2009) 1064-1068, http://dx.doi.org/10.1016/j/cnsnc.2008.05.003/.

[14] A. Aziz, *Hydrodynamic and thermal slip flow boundary layers over a flat plate with constant heat flux boundary condition*, Comm. Non. Sci. Num. Sim. 15 (2009) 573-580, http://dx.doi.org/10.1016/j.cnsns.2009.04.026/.

[15] C-H. Chen, *Magneto-hydrodynamic mixed convection of a power-law fluid past a stretching surface in the presence of thermal radiation and internal heat generation/absorption*, Int. J. Non-Linear Mechanics 44 (2009) 596-603, http://dx.doi.org/10.1016/j.ijnonlinmec.2009.02.004/.

[16] H-T, Chen, C-K. Chen, *Natural convection of a non-Newtonian fluid about a horizontal cylinder and a sphere in a porous medium*, Int. Comm. Heat Mass Transfer 15 (1988) 605-614, http://dx.doi.org/10.1016/0735-1933(88)90051-6/.

[17] S. D. Dhole, R. P. Chhabra, V. Eswaran, *Forced convection heat transfer from a sphere to non-Newtonian power law fluids*,

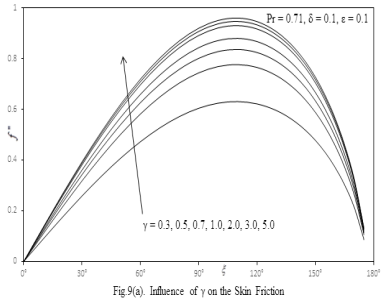

Figure 15: .

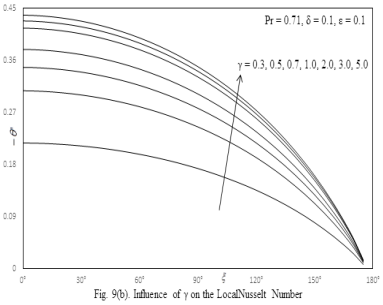

Figure 16: .

AIChemE J. 52 (2006) 3658-3667, http://dx.doi.org/10.1002/aic.10983/.

[18] N. T. M. Eldabe, S. N. Sallam, M. Y. Abouzeid, *Numerical study of viscous dissipation effect on free convection heat and mass transfer of MHD non-Newtonian fluid flow through a porous medium*, J. Egy. Math Soc. 20 (2012) 139-151, http://dx.doi.org/10.1016/j.joems.2012.08.013/.

[19] D. Gupta, L. Kumar, O. Anwar, B. Singh, *Finite element simulation of mixed convection flow of micropolar fluid over a shrinking sheet with thermal radiation*, Proc. IMechE. Part E: J Process Mechanical Engineering 228 (2014) 61-72, http://dx.doi.org/10.1177/0954408912474586/.

[20] T. Hayat, Z. Iqbal, M. Qasim, S.Obaidat, *Steady flow of an Eyring Powell fluid over a moving surface with convective boundary conditions*, Int. J. Heat and Mass Transfer 55 (2012) 1817-1822, http://dx.doi.org/10.1016/j.ijheatmasstransfer.2011.10.046/.

[21] H. B. Keller, *Numerical methods in boundary-layer theory*, Ann. Rev. Fluid Mech., 10, 417-433 (1978)

[22] A. Ishak, *Similarity solutions for flow and heat transfer over a permeable surface with convective boundary condition*, Appl. Math. Comput. 217 (2010) 837-842, http://dx.doi.org/10.1016/j.amc.2010.06.026/.

[23] T. Javed, A. Naliz, M. Sajid, *Flow of an EyringPowell non-Newtonian fluid over a stretching sheet*, Chem Eng Commun. 200 (2013) 327-336, http://dx.doi.org/10.1080/00986445.2012.703151/.

[24] M. Keimanesh, M. M. Rashidi, A. J. Chamkha, R. Jafari, *Study of a Third Grade Non-Newtonian Fluid Flow between Two Parallel Plates Using the MultiStep Differential Transform Method*, Computers and Mathematics with Applications 62 (2011) 2871-2891.

[25] M. Kumari, G. Nath, *Steady mixed convection stagnation-point flow of upper convected Maxwell fluids with magnetic field*, Int. J. Nonlinear Mechanics 44 (2009) 1048-1055 http://dx.doi.org/10.1016/j.ijnonlinmec.2009.08.002/.

[26] O. D. Makinde, P. O. Olanrewaju, *Buoyancy effects on thermal boundary layer over a vertical plate with a convective surface boundary condition*, Trans. ASME J. Fluids Eng. 132 (2010) 502-506.

[27] O. D. Makinde, A. Aziz, *MHD mixed convection from a vertical plate embedded in a porous medium with a convective boundary condition*, Int. J. Therm. Sci. 49 (2010) 1813-1820, http://dx.doi.org/10.1016/j.ijthermalsci.2010.05.015/.

[28] O. D. Makinde, K. Zimba, O. Anwar, *Numerical study of chemically-reacting hydromagnetic boundary layer flow with Soret/Dufour effects and a convective surface boundary condition*, Int. J. Thermal and Environmental Engineering 4 (2012) 89-98, http://dx.doi.org/10.5383/ijtee.04.01.013/.

[29] M. Y. Malik, A. Hussain, S. Nadeem, *Boundary layer flow of an EyringPowell model fluid due to a stretching cylinder with variable viscosity*, Scientia Iranica, Trans B: Mech Eng. 20 (2013) 313-321, http://dx.doi.org/10.1016/j.scient.2013.02.028/.

[30] M. Miraj, M. A. Alim, L. S. Andallah, *Effects of viscous dissipation and radiation on magnetohydrodynamic free convection flow along a sphere with joule heating and heat generation*, Thammasat Int. J. Science and Technology 16 (2011).

[31] M. M. Molla, S. C. Saha, *The effect of temperature dependent viscosity on MHD natural convection flow from an isothermal sphere*, Journal of Applied Fluid Mechanics 5 (2012) 25-31.

[32] M. Norouzi, M. Davoodi, O. Anwar, A. A. Joneidi, *Analysis of the effect of normal stress differences on heat transfer in creeping viscoelastic Dean flow*, Int. J. Thermal Sciences 69 (2013) 61-69, http://dx.doi.org/10.1016/j.ijthermalsci.2013.02.002/.

[33] R. E. Powell, H. Eyring, *Mechanism for relaxation theory of viscosity*, Nature 7 (1944) 427-428, http://dx.doi.org/10.1038/154427a0/.

[34] K. V. Prasad, P. S. Datti, B. T. Raju, *Momentum and heat transfer of a non-Newtonian Eyring-Powell fluid over a non-isothermal stretching sheet*, Int. Journal of Mathematical Archive 4 (2013) 230-241.

[35] V. R. Prasad, B. Vasu, O. Anwar, D. R. Parshad, *Thermal radiation effects on magnetohydrodynamic free convection heat and mass transfer from a sphere in a variable porosity regime*, Comm. Nonlinear Science Numerical Simulation 17 (2012) 654-671, 2012, http://dx.doi.org/10.1016/j.cnsns.2011.04.033/.

[36] J. N. Potter, N. Riley, *Free convection from a heated sphere at large Grashof number*, J. Fluid Mechanics 100 (1980) 769-783.

[37] A. Prhashanna, R. P. Chhabra, *Free convection in power-law fluids from a heated sphere*, Chem. Eng. Sci. 65 (2010) 6190-6205, http://dx.doi.org/10.1016/j.ces.2010.09.003/.

[38] V. Ramachandra Prasad, A. Subba Rao, N. Bhaskar Reddy, B. Vasu, O. Anwar, *Modelling laminar transport phenomena in a Casson rheological fluid from a horizontal circular cylinder with partial slip*, Proc IMechE Part E: J Process Mechanical Engineering 227 (2013)309-326 http://dx.doi.org/10.1177/0954408912466350/.

[39] M. M. Rashidi, M. T. Rastegari, M. Asadi, O. Anwar Beg, *A Study of Non Newtonian Flow and Heat Transfer over a Non Isothermal Wedge Using the Homotopy Analysis Method*, Chemical Engineering Communications 199 (2012) 231-256.

[40] A. M. Siddiqui, A. A. Farooq, Badcock, *Two analytical methods applied to study thin film flow of an Eyring-Powell fluid on a vertically moving belt*, Applied Mathematical Sciences 7 (2013) 3469-3478, http://dx.doi.org/10.12988/ams.2013.34200/.

[41] S. V. Subhashini, N. Samuel, I. Pop, *Double-diffusive convection from a permeable vertical surface under convective boundary condition*, Int. Commun. Heat Mass Transfer 38 (2011) 1183-1188,http://dx.doi.org/10.1016/j.icheatmasstransfer.2011.06.006/.

[42] M. Subhas Abel, P. S. Datti, N. Mahesha, *Flow and heat transfer in a power-law fluid over a stretching sheet with variable thermal conductivity and non-uniform heat source*, Int. J. Heat Mass Transfer 52 (2009) 2902-2913, http://dx.doi.org/10.1016/j.ijheatmasstransfer.2008.08.042/.

[43] G. Swapna, L. Kumar, O. Anwar, B. Singh, *Finite element analysis of Radiative mixed convection Magneto-micropolar flow in a Darcian porous medium with variable viscosity and convective surface condition*, Heat Transfer Asian Research 44 (2014) 515-532.

[44] M. J. Uddin, N. H. M. Yusoff, O. Anwar, A. I. Ismail, *Lie group analysis and numerical solutions for non-Newtonian Nanofluid flow in a porous medium with internal heat generation*, Physica Scripta, Vol. 87, No. 2, 025401. 2013. doi: http://dx.doi.org/10.1088/0031-8949/87/02/025401/.

[45] Y. L. Zhang, K. Vairavamoorthy, *Analysis of transient flow in pipelines with fluidstructure interaction using method of lines*, Int. J. Num. Meth. Eng. 63 (2005) 1446-1460, http://dx.doi.org/10.1002/nme.1306/.

S. Abdul Gaffar was born in Madanapalle, Chittoor District, Andhra Pradesh, India, in May, 1982. He completed a First Class Masters of Sciences, degree in Mathematics (2004) from Sri Venkateswara University, Tirupati, and is pursuing PhD in Flow and Heat transfer of Casson Fluid on Boundary Layer (Registered in 2011), JNT University Anantapur, Anantapuramu. He worked as lecturer in the Department of Mathematics, Bapatla College of Engineering, India, for one year (2004). Later from May 2007 to April 2013, he was the Assistant Professor for five years in the Department of Mathematics, Mother Theresa Institutions. From 2013 to till date he is working as Lecturer in the Department of Mathematics, Salalah college of Technology, Salalah, Oman. He has published in excess of 18 journals in peer reviewed journals. He is currently engaged in different non-Newtonian fluids over different curved bodies.

Professor Dr. V. Ramachandra Prasad was born in Madanapalle, Chittoor District, Andhra Pradesh, India, in July, 1968. He completed a Distinction Class Masters of Sciences, degree in Mathematics (1994) from Osmania University, Hyderabad, and a PhD in Radiation and Mass Transfer Effects on connective flow past a vertical plate (2003), both from Sri Venkateswara University, Tirupati. He then worked as lecturer in the Department of Mathematics, Besant Theosophical College, Madanapalle, India, for seven years (19942001). From May 2001 to April 2007, he was the Assistant Professor for six years in the Department of Mathematics, in Madanapalle Institute of Technology and Science. Later from May 2007 to April 2009 worked as Associate Professor, in the Department of Mathematics, Madanapalle Institute of Technology and Science, Madanapalle, India. From May 2009 to till date he is working as Professor in the Department of Mathematics, Madanapalle Institute of Technology and Science, Madanapalle, India. He has authored Radiation effects on Convective Flow Past a Vertical Plate: Radiation and Mass Transfer Effects on Convective Flow Past a Vertical Plate (Lambert, Germany, 2010), Thermo-Diffusion and Diffusion-Thermo Effects on Boundary Layer Flows (Lambert, Germany, 2011) and Walters˙B Viscoelastic flow Past a Vertical Plate: Numerical Study of Unsteady Free Convective Heat and Mass Transfer in a Walters˙B Viscoelastic Flow Past a Vertical Plate (Lambert, Germany, 2012). He has published in excess of 50 journal articles. His research has also been presented at over 13 conferences. He is currently engaged in different non-Newtonian fluids over different curved bodies.

Dr. E. Keshava Reddy, presently working as Professor of Mathematics in JNT University College of Engineering Anantapur. He has 15 years of experience in teaching and 11 years in research. He completed his PhD degree in Mathematics from prestigious University Banaras Hindu University Varanasi. His areas of interest include Functional Analysis, Optimization Techniques, Data Mining, Neural Networks, Fuzzy Logic and Optimization techniques. He guided 2 PhD, 1MPhil and has published more than 35 Research papers in National and International Journals and Conferences. He authored 06 books on Engineering Mathematics and Mathematical Methods for various universities. He worked as Chairman of Board of studies for the faculty of Mathematics for JNTUA both at UG level and at PG level. Presently he is the chairman, PG Board of studies for Mathematics of JNTUA. He is a member of Board of Studies for Mathematics of various universities.

Int. J. of Industrial Mathematics **Vol. 8, No. 2** (2014)

Non-Newtonian thermal convection of eyring-powell fluid from an isothermal sphere with biot number effects

S. Abdul Gafar, V. Ramachandra Prasad, E. Keshava Reddy

روش FGP برای برنامه ریزی کسری تابع هدف درجه دوم

چکیده:

در این مقاله یک روش کارا برای حل معادلات انتگرال تصادفی ولترای نوع دوم به کمک بسط تیلور معرفی می شود. این روش معادله انتگرال تصادفی ولترای نوع دوم را به یک معادله دیفرانسیل خطی تصادفی معمولی با نیاز به شرایط مرزی مشخص تبدیل می کند. برای تعیین این شرایط مرزی از تکنیک انتگرال گیری استفاده می شود. این تکنیک یک تقریب ساده و بسته از جواب معادله انتگرال تصادفی ولترای نوع دوم ارائه می دهد. امید ریاضی فرایند تقریب محاسبه می شود و چندین مثال عددی برای نشان دادن کارایی این روش ارائه شده است.